

Sequence-dependent B-A transitions in DNA *in silico*: Electrostatic condensation mechanism

Alexey K. Mazur

CNRS UPR9080, Institut de Biologie Physico-Chimique,
13, rue Pierre et Marie Curie, Paris, 75005, France

Dynamics of the polymorphic A \leftrightarrow B transitions in DNA is compared for two polypurine sequences, poly(dA).poly(dT) and poly(dG).poly(dC), long known to exhibit contrasting properties in experiments. In free molecular dynamics simulations reversible transitions are induced by changing the size of a water drop around DNA neutralized by Na⁺ ions. In poly(dG).poly(dC) the B \leftrightarrow A transitions are easy, smooth and perfectly reversible. In contrast, a B \rightarrow A transition in poly(dA).poly(dT) dodecamer fragment could not be obtained even though its A-form is stable under low hydration. Normal B \rightarrow A transitions are observed, however, in long poly(dA).poly(dT) stretches flanked by GC pairs. An intermediate range of hydration numbers is identified where opposite transitions are observed in the two dodecamer fragments, namely, A \rightarrow B in poly(dA).poly(dT) and B \rightarrow A in poly(dG).poly(dC). With hydration numbers close to the stability limit of the B-form, the two sequences exhibit qualitatively different counterion distributions, with a characteristic accumulation of Na⁺ ions next to the opening of the minor groove in poly(dA).poly(dT). This difference can explain an increased persistence of poly(dA).poly(dT) DNA towards A-form in crystalline and amorphous fibers as compared to solution conditions. The good overall agreement with experimental data corroborates the general role of the electrostatic condensation mechanism in the A/B polymorphism in DNA.

Introduction

Reversible transitions between the A and B forms of DNA¹ represent one of the modes for governing protein-DNA interactions, with the B-form as the dominant biological conformation and the A-form as a high energy state adopted temporarily for different purposes^{2,3}. These transitions can be induced in several ways *in vitro*^{4,5,6,7} and they were extensively studied in the recent decades. However, a number of interesting issues are still unclear including the underlying molecular mechanisms and the driving forces. Different theoretical approaches were applied in this field during its long history^{8,9,10,11,12}. In the recent years realistic molecular dynamics (MD) simulations of A \leftrightarrow B transitions became possible including relevant explicit solvent environment^{13,14,15,16,17,18,19,20}. Despite the limited duration of trajectories and some force field artifacts²¹, these studies helped to get new insights in the putative molecular mechanisms of the DNA A/B polymorphism. A new approach recently found in this field consists in using small water drops as solvent shells around DNA fragments²². By changing the size of the drop, reversible A \leftrightarrow B transitions can be induced, with hydration numbers in rough agreement with experimental values²⁰.

The water drop simulation approach is the first and the only presently known technique to obtain reversible B \leftrightarrow A transitions in DNA *in silico*. The established mechanism of such transitions essentially consist in an intra-duplex electrostatic condensation of the two DNA strands. With the drop size gradually reduced, the equilibrium is shifted towards the A-form due to inversion of electrostatic interactions across the major DNA groove when the local cation concentration exceeds a certain

transition level. The important role of this particular type of interactions is well established in the earlier literature^{23,24}. Similar B \rightarrow A transitions were observed experimentally in poly(dG).poly(dC) fragments with multivalent cations bound in the major groove²⁵, which could be reproduced in simulations¹⁶. This mechanism is perhaps generally responsible for the A/B polymorphism, but a number of other ideas concerning its nature are also being discussed. Among them one can mention the factor of economy of hydration of the sugar phosphate backbone²⁶, the base stacking interactions⁹ and the hydrophobic effect^{11,27}. It is interesting, therefore, to know if the A \leftrightarrow B transitions in water drop simulations that are relatively simple to study and rationalize are really similar to those in experimental conditions. To this end we should check if different aspects of the A/B polymorphism *in silico* correspond to the experimental results for the most part obtained for DNA in fiber crystals under low relative humidity and in concentrated solutions of some non-polar solvents. Among such aspects the sequence dependent nature of the A/B polymorphism is perhaps most intriguing and well documented.

Sequence effects upon the B \rightarrow A transition attract long-standing interest. In fiber crystals, DNAs with different regular sequences often exhibit dissimilar capacities to adopt the two forms^{5,28}. The same trends are observed in solution, moreover, here the pattern revealed is much richer because a large variety of sequences could be probed, with their propensities towards A- and B-forms measured quantitatively². It was shown that, during transitions in long natural DNA, different regions switch between the two forms in a complex sequence specific order²⁹. The A/B-phlicity of different base pair steps and triplets was examined systematically

in synthetic fragments. It could be parametrized and used successfully for predicting the properties of mixed sequences^{2,30,31}. All these effects certainly originate from interactions between stacked bases and some of them could be rationalized^{9,10,11}.

The measured A/B propensities appear such that consecutive base pair steps tend to compensate one another, therefore, generic DNA sequences commonly are neither A- nor B-philic³¹. A strong difference is observed, however, between the stretches of consecutive guanines and adenines (G-tracts and A-tracts, respectively). Double helical DNA fragments with these two sequences exhibit contrasting physico-chemical properties as established by a number of different methods^{5,28,32,33,34,35,36,37,38,39,40,41,42,43,44,45,46}. A systematic review of these data has been published recently⁴⁷. In G-tracts, the B→A transition is very easy. The poly(dG).poly(dC) DNA is generally prone to adopt the A-DNA conformation in conditions where random sequences stay firmly in the B-form^{5,36,40}. In contrast, in A-tracts, the B→A transition is particularly difficult^{5,40,46}. Notably, a B→A transition was never observed in fiber crystalline poly(dA).poly(dT) because in standard transition conditions it is reportedly prone to denaturation or alternative transformations^{5,28}. Solvent cations were found to bind in the major grooves of G-tracts and in the minor grooves of A-tracts and not vice versa, which is probably related and perhaps responsible for the A/B propensities of these sequences^{47,48}. This remarkable physico-chemical difference is particularly important in the context of the intriguing roles of A-tracts and G-tracts in the genome functioning. Various A-tract sequences are overrepresented in both prokaryotic and eukaryotic genomes⁴⁹. They are long known to cause DNA curvature in solution that can affect binding to proteins and formation of nucleosomes^{50,51}. Long G-tracts are also widespread in eukaryotic as well as archaeobacteria genomes⁵².

Here we report about the results of systematic simulation studies of A↔B transitions in a series of DNA fragments with these two characteristic sequence motifs. The established experimental preferences of A- and G-tracts towards B and A forms, respectively, are qualitatively well reproduced. In poly(dG).poly(dC) dodecamer, the B→A transition is easy, smooth and perfectly reversible. In contrast, a B→A transition in similar poly(dA).poly(dT) fragment could not be obtained even though its A-form was found stable under low hydration. At the same time, normal B→A transitions are observed in long poly(dA).poly(dT) stretches flanked by GC pairs. An intermediate range of hydration numbers is found where opposite transitions are observed in the two dodecamer fragments, namely, A→B in poly(dA).poly(dT) and B→A in poly(dG).poly(dC). These results agree with the assumed similarity of the A↔B transitions in experiment and in water drop simulations. It appears that, with hydration numbers close to stability of the B-form, these two fragments have qualitatively different

counterion distributions, with a characteristic accumulation of Na⁺ ions next to the opening of the minor groove in poly(dA).poly(dT). In fibers, these ion positions can be additionally stabilized by intermolecular contacts, which would explain an increased persistence of poly(dA).poly(dT) DNA towards A-form in crystalline and amorphous fibers as compared to solution conditions.

Results

Comparative dynamics of A↔B transitions

Fig. 1 shows the sugar pucker dynamics in a series of representative trajectories of G12. Transitions from C2'-endo to C3'-endo are observed starting already from HN42. At first they occur only in the purine strand and for HN33 and HN29 an intermediate state is obtained with this strand almost entirely in the C3'-endo conformation. A complete transition to A-form is reached in the middle of the duplex starting from HN25. This transition midway point is similar to that reported for the dodecamer CGCGAATTCGCG²⁰. However, here the A-DNA backbone appears at much higher hydration numbers and, as a result, the transition looks smoother and less cooperative. Moreover, the final A-DNA structure spreads from the center almost to entire fragment so that the B-philicity of the DNA ends, generally observed in experiments and calculations^{20,56}, is less significant. All this agrees well with the known A-philicity of the poly(dG).poly(dC) DNA⁵⁷.

Fig. 2 shows a titration-like pattern of these transitions as followed by different structural parameters. Different traces all exhibit S- or Z-shaped profiles sometimes with a very distinct transition zone⁵⁸. The A-DNA structures observed under low hydration are very close to the canonical conformation, with final RMSD values below 2 Å. In contrast, under the highest hydration, an underwound B-DNA is observed with a strong bias towards A-form. Similar deviations were reported earlier by others^{59,60,61} and they are partially due to the known negative force-field bias of the Twist⁶². The A↔B transitions for G12 are easily achieved in both directions and the points in Fig. 2 corresponding to the transition zone could be reproduced in alternative simulations starting from the A-DNA state.

Similar results for A12 are shown in the next two figures. The most striking difference from G12 could not be shown here, namely, that we failed to obtain a B→A transition for this fragment in spite all efforts. At the same time, the A-form was perfectly stable under low hydration and, for HN21 and higher numbers, the A→B transitions passed without problems. Therefore, for Fig. 3, the trajectories chosen all started from the A-DNA conformation and we may add that, with the exception of HN13 and HN17, the B-DNA dynamics was also stable and converged to the same structures. Comparison of Fig. 3 with Fig. 1 readily reveals a stretch of hy-

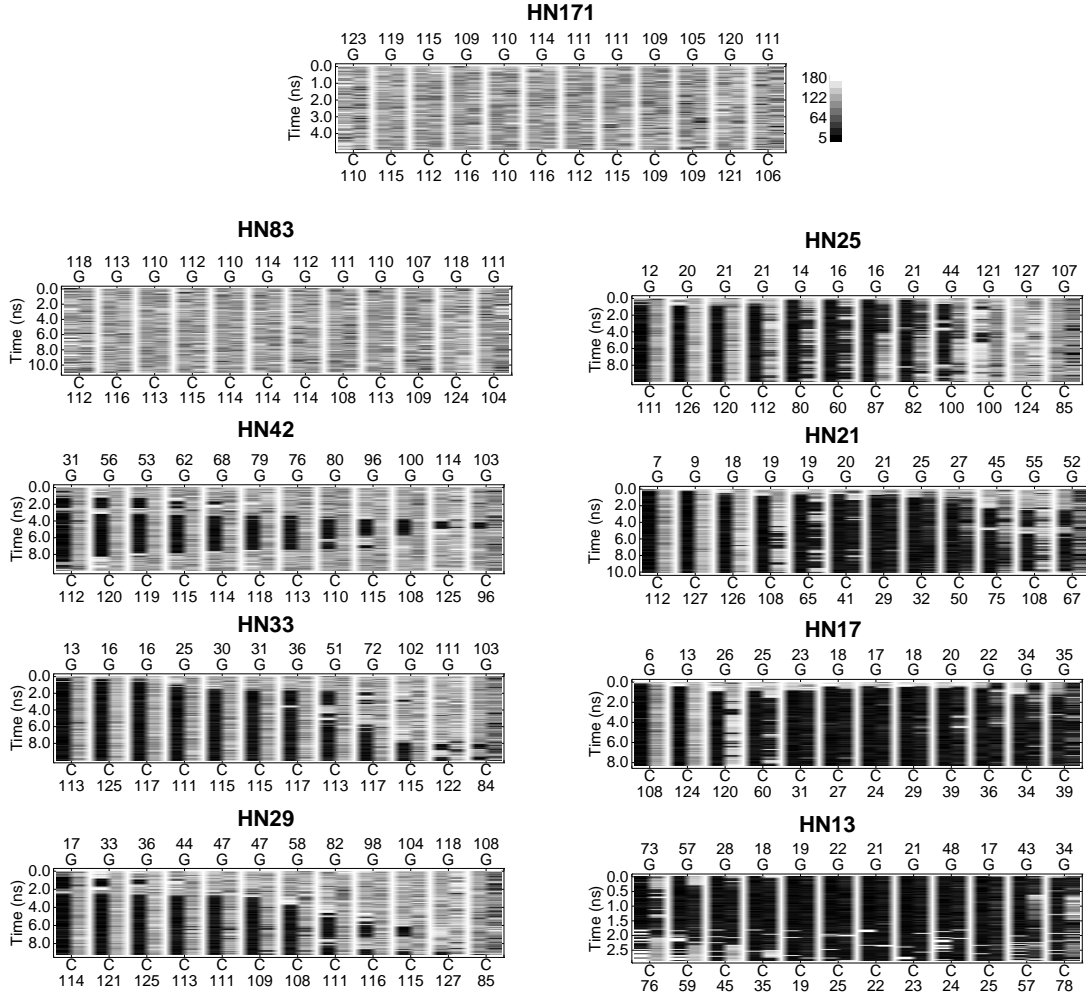


FIG. 1: Dynamics of sugar pucker pseudorotation⁵³ in G12 under different hydration numbers. The boundary pucker values (ca 0° and 180°) are assigned the black and the white colors, respectively, with intermediate values mapped linearly to the gray scale levels. Each base pair step is characterized by a column consisting of two sub-columns, with the left sub-columns referring to the sequence written above in 5'-3' direction from left to right with the time averaged phases given on top. The right sub-columns refer to the complementary sequence shown below together with the corresponding time averaged phases. All trajectories shown in this figure started from the B-DNA state except the HN13. The last simulation started from the final state of HN17 because the original B-DNA state is unstable and prone to collapse under that low hydration.

hydration numbers were opposite transitions are observed in G12 and A12, that is the simulations reproduce the expected relative difference between these two fragments as regards their preference towards A- vs B-DNA.

Fig. 4 exhibits a pattern qualitatively similar to that in Fig. 2 with a few exceptions. Again the computed A-DNA structures are very close to the canonical conformation, but in this case the computed B-DNA are also relatively similar to the canonical one, even though the twist remains strongly underestimated. These traces were obtained by increasing hydration as shown in Fig. 3. In the opposite sense they could be also reproduced except for the hydration numbers below 21. In conditions HN17 and HN13, repetitive trajectories of A12 starting from B-DNA resulted in opening of terminal base pairs

followed by irregular deformations that have been interpreted as beginning of denaturation. Interestingly, when this limiting hydration is approached from the right in Fig. 4 the data show no trend towards the A-form. Instead some parameters are nearly stable while the other even exhibit a trend in an opposite direction, suggesting that the B-DNA structure is progressively stabilized before the eventual base pair opening and collapse.

Evolution of Na^+ distributions around DNA

The distributions of counterions around DNA are compared for G12 and A12 in Fig. 5. The patterns shown here are interpreted as follows. The duplexes are entirely

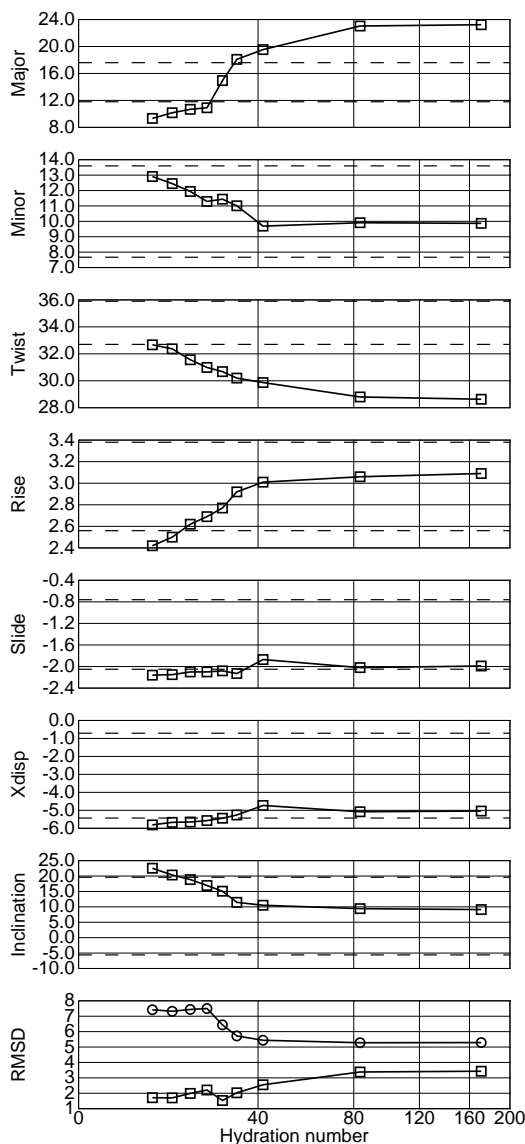


FIG. 2: Quasi-static pattern of A \leftrightarrow B transitions for G12 as monitored by different structural parameters. For each hydration number, a long MD trajectory was computed and the last 1 ns average structures were analyzed to obtain the necessary values. The two top plates show the average groove widths measured as described elsewhere^{20,54}. Several helical parameters are all computed by Curves⁵⁵, with the local values for the Slide and global ones for the rest. The RMSD from the canonical A and B-DNA conformations is shown by circles and squares, respectively. All distances are in angströms and angles in degrees. The dotted lines indicate canonical A- and B-DNA levels.

covered by water, therefore, the radial distribution of water oxygens shows the evolution of the available volume not occupied by DNA. Even though the relative sizes of water and Na⁺ are not identical, these profiles give a rough estimate of free space that can be sampled by ions, and, in the absence of specific DNA-ion interactions, the solid and dotted traces in Fig. 5 should have similar

peak positions. In contrast, radial zones of strong Na⁺-DNA interaction produce strong separate peaks. Note also that the height of each peak in a cylindrical distribution should be multiplied by the corresponding distance when their relative weights are estimated.

The characteristic distributions for B-DNA are best seen in the several top plates of A12. It does not differ from similar distributions earlier reported for CGCGAATTCGCG²⁰. The three broad water peaks at approximately 4, 8 and 12.5 Å correspond, respectively, to the first water layer in the major groove, the next few layers in both major and minor grooves and the bulk water outside DNA radius which is about 10 Å for both A- and B-DNA. The first Na⁺ peak at 5 Å is a sum of several different contributions. It involves ions that interact with bases directly in depth of the minor groove as well as those in contact with N7 atoms of purine bases in the major groove. Mobile ions in the second hydration shell in the major groove also contribute to this peak because Na-OW distances are somewhat shorter than OW-OW ones. In cylindrical distributions in Fig. 5 these qualitatively different contributions could not be resolved and that is why Na⁺ peaks at 5 Å are found in B- as well as A-DNA distributions and often vary in height. The outer peak at 12.5 Å includes highly mobile ions around DNA involved in non-specific phosphate screening. Its prominent part that becomes less mobile under low hydration corresponds to Na⁺ positions along the minor groove between the two phosphate strands. Finally, an intermediate peak at approximately 8 Å is generally produced by mobile ions in the minor groove. Ion entering into the minor groove was relatively rare, perhaps because the starting Na⁺ distributions sampled only outer positions, which explains why such peaks are less well reproduced between the trajectories.

The characteristic A-DNA distributions can be seen in the bottom plates of A12 as well as in many plates of G12. In this case the center of the DNA cylinder is filled with water and, consequently, accessible for ions. Most of them rest inside the DNA radius. As regards the relative weights, the most prominent peak is found at 10 Å and it corresponds to Na⁺ sandwiched between the opposite phosphate groups in the opening of the major groove. It is the accumulation of counterions at this region that causes the B \rightarrow A transition²⁰.

For G12 even under high hydration the Na⁺ distribution is rather different from typical B-DNA. These structures have a strong negative Xdisp, therefore, the helical axis is shifted to the major groove and is accessible to water and ions. Even though in HN82 most of Na⁺ stay outside the DNA radius their population inside the major groove is already significant. With hydration numbers reduced, the counterions are progressively pushed inside DNA. The Na⁺ peak corresponding to the opening of the major groove emerges gradually and starting from HN25 it becomes predominant. All this corresponds well to the relatively smooth B \rightarrow A transition characterized above in Fig. 1 and Fig. 2. The A12 patterns in the right

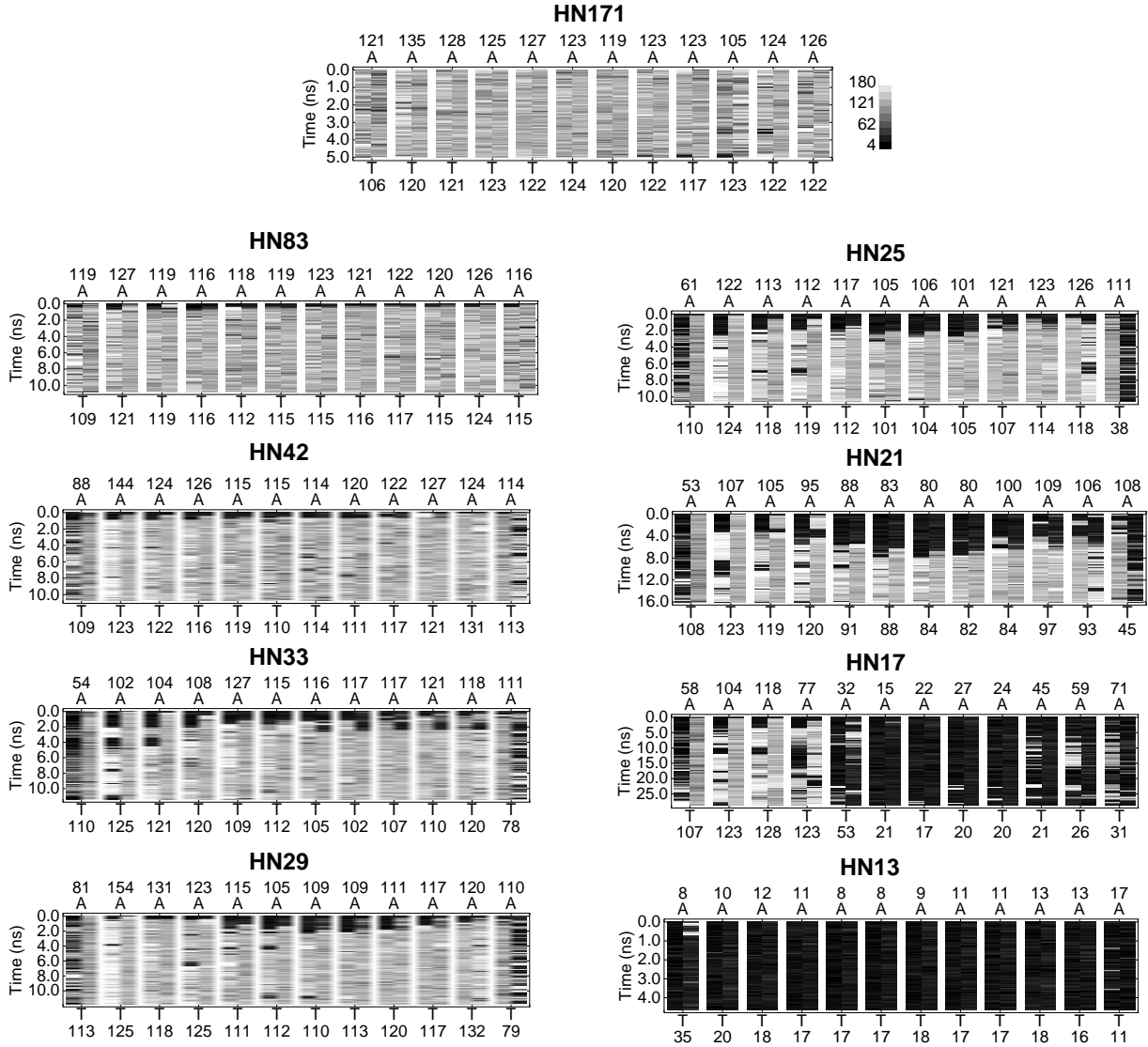


FIG. 3: Dynamics of sugar pucker pseudorotation in A12 under different hydration numbers. All trajectories shown in this figure started from the A-DNA state .

column are radically different. In this case both water and Na^+ distributions retain the characteristic B-DNA shapes even with the hydration number reduced to 21. The ions are not pushed inside DNA when the outer water shell is reduced, and the Na^+ peak at 12.5 Å remains dominant.

An evident demonstration of the distinction between these two DNA fragments as regards their relative capacities to adopt A- and B-forms is given in Fig. 6 where the snapshots are shown for A12 and G12 at the end of dynamics simulated in drops of the same size (HN25). These structures and the counterion distributions confirm the main aspects of dynamics illustrated by previous figures. For A12 we have a B-DNA with a narrow minor groove near both ends and a widening in the middle. A

large number of the Na^+ ions stays outside DNA in front of the minor groove. In contrast, G12 gives a typical A-DNA conformation with a layer of Na^+ sandwiched between the opposite phosphate groups in the narrow major groove. This "electrostatic sandwich" provides the main driving force of the B→A transition according to the condensation mechanism^{15,20,24}.

Persistence of poly(dA).poly(dT) DNA to A-form

A series of additional calculations was carried out in order to check the origin of the A12 persistence with respect to A-DNA. It was possible that, the poly(dA).poly(dT) was intrinsically unstable with respect to base pair open-

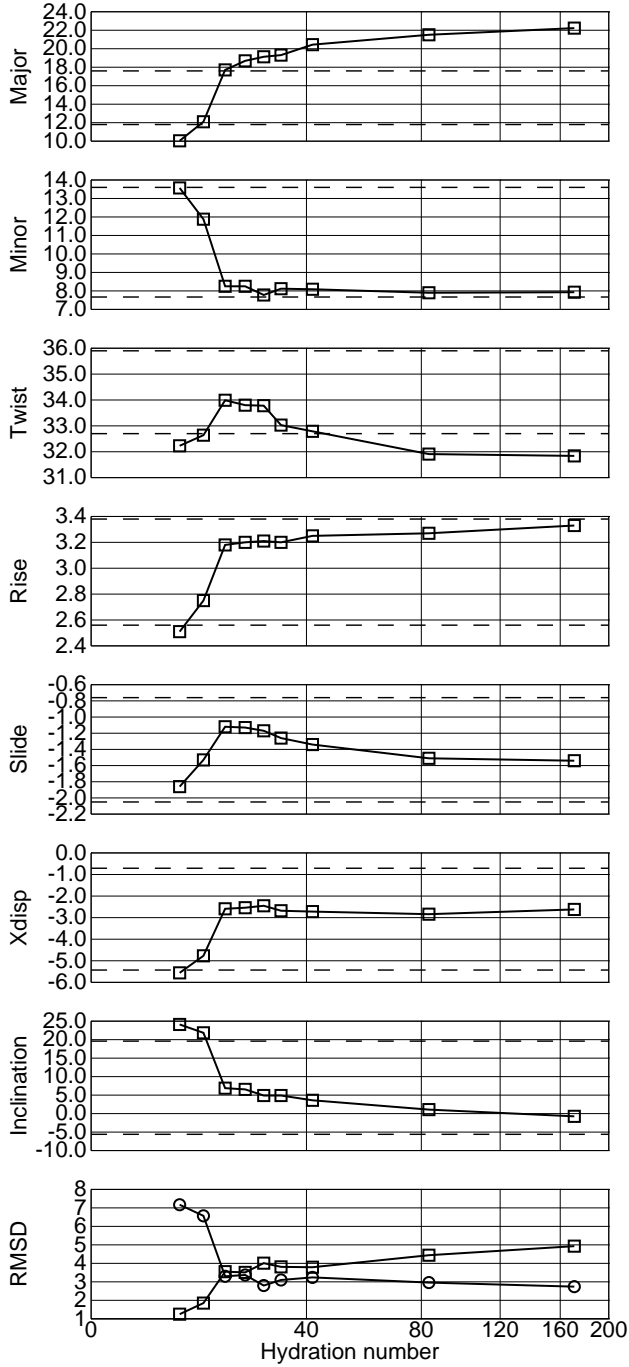


FIG. 4: Quasi-static pattern of $A \leftrightarrow B$ transitions for A12. The notation is as in Fig. 2.

ing during the $B \leftrightarrow A$ transition due to mechanical stretching of base pairs under intermediate hydration numbers. In solution experiments, DNA commonly exhibits reduced thermostability under intermediate alcohol concentrations⁶³. It can even denature and then renature when the water activity is further reduced⁶⁴. To probe this transitional instability several long trajectories were run for A-DNA close to the intermediate hy-

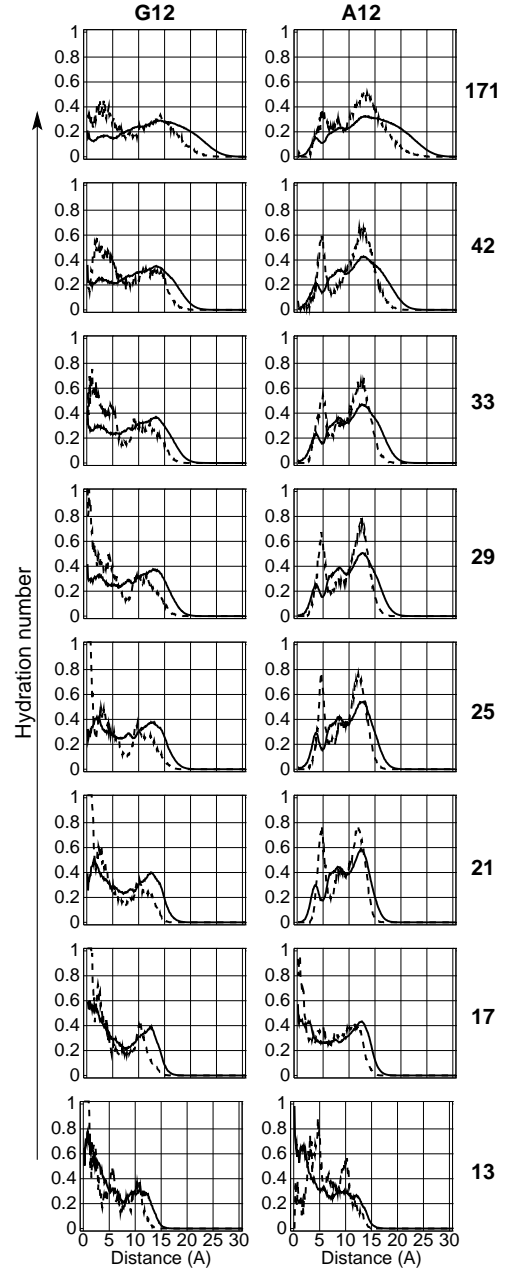


FIG. 5: Cylindrical radial distribution functions for water oxygens (solid lines) and Na^+ ions (dashed lines) around G12 and A12. DNA structures saved in the last nanosecond of dynamics together with surrounding water and counterions were superimposed with the canonical B-DNA with the global coordinate OZ direction as the common helical axis. The Na^+ ions and water oxygens were counted in coaxial 0.1 Å thick cylinders. The distributions are volume normalized, that is scaled with a factor of $1/r$, and the final plots were area normalized. The corresponding hydration numbers are shown on the right.

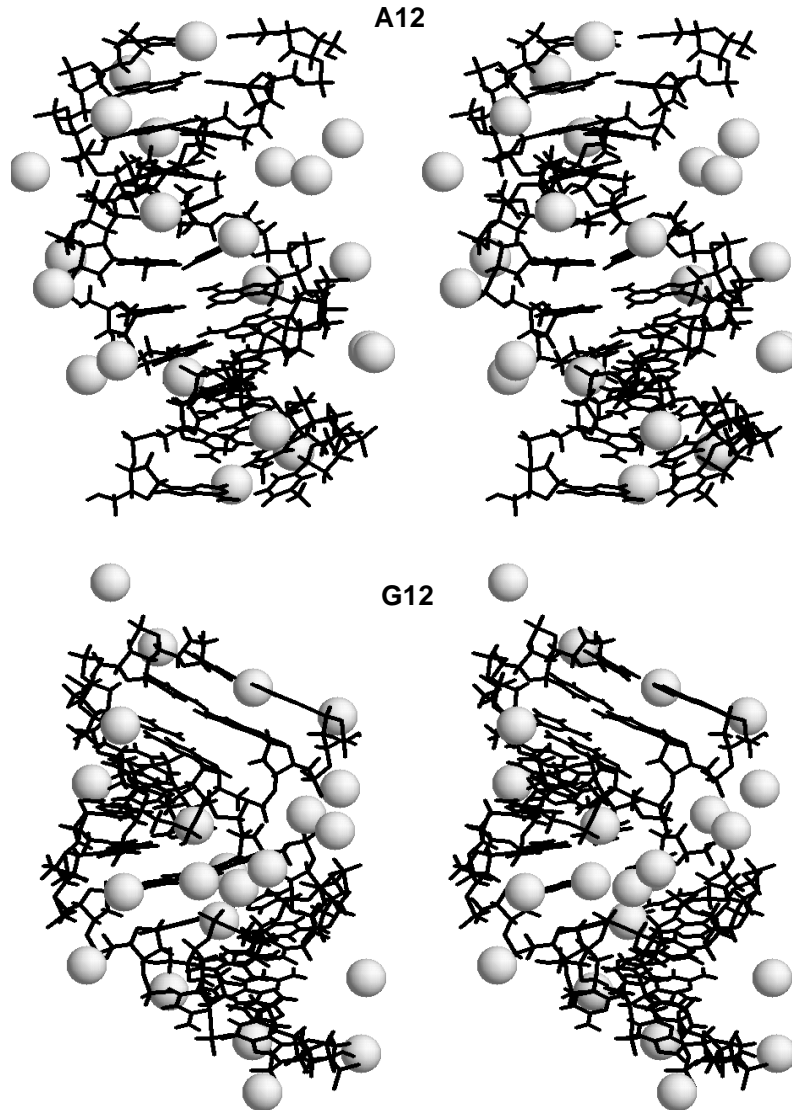


FIG. 6: Stereo snapshots of the final computed states of A12 and G12 obtained with the same drop size corresponding to the hydration number of 25. The Na⁺ ions are shown by spheres.

dration. Other simulations involved forced opening of one base pair to check if this could induce denaturation. In all these tests the A-DNA remained stable.

The opening of terminal base pairs could also result from kinetic instability of B-DNA when it is suddenly transferred under low hydration. Such an opening is sometimes observed even for G12 when trajectories start from B-DNA in HN13. To check this possibility, simulations were continued from the final B-DNA state of the HN21 trajectory, with the amount of water reduced smoothly in several steps by removing each time only molecules not in contact with ions. This slow "evaporation" also led to opening of a terminal base pair under an intermediate hydration, with the structure remaining in the B-form.

Finally, it was possible that the opening of terminal

base pairs masks the B→A transition kinetically, that is the molecule just cannot stay intact long enough for the transition to occur. To check this the two opposite terminal AT base pairs were replaced by GC and dynamics was simulated starting from B-DNA in HN17 and HN13 water drops. In these simulations no base pair opening was observed. For HN17 two trajectories were computed of 11 and 7 ns, respectively, with different random initial distributions of counterions. In both cases the duplex remained firmly in the B-DNA state. For HN13 the trajectory was continued to 5.5 ns. During this time water started to leave the minor groove and the duplex suffered irregular deformations that drove it to a shrunk collapsed structure with partially closed grooves, and yet the transition to the A-form did not occur.

The foregoing pattern is in a remarkable correspondence with the well documented poly(dA).poly(dT) phobicity towards the A-form^{5,28}. Unfortunately, this finding does not yet mean that a simple mechanism of this resistance can be readily extracted from simulations. It appeared that the B→A transitions in poly(dA).poly(dT) fragments become possible when the chain length is increased. In a 16-mer fragment of poly(dA).poly(dT) under HN17, opening of several terminal base pairs at both ends was also observed, however, this was accompanied by a B→A transition in a few central residues. When the two terminal base pairs at the opposite ends were replaced with GC the resulting 16-mer fragment CGAAAAAAAAAAGC under the same hydration showed a normal B→A transition in the middle 12-mer A-tract with the same general features as described before. With the length of the A-tract further increased to 18 base pairs, a B→A transition could also be obtained under HN21.

Discussion

The experimental studies of the B/A polymorphism in solution earlier revealed a surprisingly complex pattern of the double helical DNA behavior depending upon its sequence as well as environment conditions such as the water activity, the temperature, the type and the concentration of counterions. Perhaps not all effects observed *in vitro* are biologically relevant, but the exceptional role of the DNA molecule makes any information concerning its properties potentially important. Unfortunately, a number of intriguing experimental observations in this field could not be accurately interpreted in terms of DNA structure because the direct NMR and X-ray methods are not always applicable and often limited in accuracy. Molecular dynamics simulations of the type described here can help to clarify some long standing issues in this domain provided that the mechanism of A↔B transitions is similar *in silico* and *in vitro*.

Under low hydration, dynamic DNA structure systematically converges to the A-form conformation that is very similar for different sequences and very close to the canonical conformation observed in fiber crystals. In contrast, a much more significant and sequence dependent divergence from experimental structures is systematically obtained for B-DNA. There is a surprising correspondence between this difference and experimental data. The high regularity and the absence of sequence effect for A-form was noticed long ago for X-ray fiber diffraction patterns⁵ and later confirmed in the ensemble of single crystal A-DNA structures⁶⁵. Thus, in both experiment and simulations, the A-form of DNA is virtually insensitive to the base pair sequence. In simulations it appears also to be relatively insensitive to the accuracy of the forcefield that do not allow MD trajectories to come closer to experimental B-DNA conformations. These observations may have a common physical origin. Notably,

they can be attributed to the A-form being dominated by the "electrostatic sandwich" in the major groove. The strong interactions of phosphate groups with metal cations effectively impose geometric constraints upon the inter-phosphate distances and suppress all other factors that might affect the overall structure. Similar types of interactions are also possible for the A-form stretches observed in complexes with proteins. In all such structures resolved by now the major groove of A-DNA is exposed to solvent whereas extensive protein DNA contacts are observed in the minor groove.

The systematic deviations of the computed B-DNA conformations from the canonical one are similar to the recent simulations for analogous sequences^{59,60,61}. The Cornell et al parameters⁶⁶ have a well documented tendency to underestimate the average helical twist⁶², and for the sequences studied here this bias is perhaps the largest. For poly(dG).poly(dC) this results in structures with very A-like helical parameters. At the same time, sugar pseudorotation dynamics samples mainly from South/East phases characteristic of B-DNA (see Fig. 1). Earlier such structures were interpreted as strongly underwound B-DNA or as A-DNA with B-like backbone^{59,60,61}. Unfortunately, it is rather difficult to tell exactly how strong is the deviation of these conformations from experimental data. They are rather different from G-tracts found in a large number of A-DNA single crystal structures. However, these structures are found in a unique A-DNA packing characterized by very special DNA-DNA interactions in wide minor grooves⁶⁷. The same trend is not seen in short G-tracts found in protein-DNA complexes. For instance, one of the resolved structures of the Y-family DNA polymerase contains a DNA fragment with an exposed GGGGG terminus⁶⁸. This G-tract features a normal B-DNA conformation with South sugar puckers and the average Twist of 34.2° rather close to that of generic B-DNA. Unfortunately, the last value is much larger than the measured solution value (ca 32.7° for long G-tracts³²) suggesting that the DNA structure may again be affected by the crystal environment. On the other hand, solution NMR and Circular dichroism (CD) studies indicate that the G-tract duplexes computed with the Cornell et al force field resemble experimental structures^{59,60}. The corresponding CD spectra are very similar to typical A-DNA suggesting that the high hydration conformation of poly(dG).poly(dC) already has an A-like base pair stacking. At the same time, the sugar phases determined by NMR are all at the South. These conformations can hardly be assigned to the A-form because a cooperative transition to a genuine A-form is still distinguishable in solution as well as in crystalline fibers although the corresponding spectral changes are small^{59,60,69}. These subtle changes can well result from a transition pattern similar to that in Fig. 2, with sugar phases switching to the North and grooves changing their width, but relatively minor shifts in helical parameters.

The poly(dA).poly(dT) conformation at the high hy-

dration limit are much closer to the canonical B-DNA structure although, in agreement with earlier reports⁷⁰, it is also underwound by ca 4° with respect to the experimental solution value^{32,33,34}. Our simulations managed to reproduce the well-documented relative A-form phobicity of this sequence in several different aspects. Notably, there is a well defined range of hydration numbers where poly(dA).poly(dT) and poly(dG).poly(dC) are stable in B- and A-forms, respectively. Dodecamer A12 resembles poly(dA).poly(dT) properties in crystalline fibers in that it refuses to go to the A-form and is prone to denaturation. At the same time, longer poly(dA).poly(dT) fragments with GC termini adopt the A-form without great problems, which agrees with experiments in solution³¹. It seems rather perplexing that a B→A transition for A12 could not be obtained in spite of the fact that its A-form was found to be perfectly stable under low hydration. It is known, however, that in some experimental conditions, the B→A transition in DNA can go via temporary condensation or denaturation⁶⁴. If the lowest energy transition pathway goes like that in our conditions, the molecular dynamics simulations would not be able to reach the final state because of the limited duration of trajectories. One should also keep in mind that the experimental B↔A transitions in DNA reportedly involve macroscopically slow relaxation phases and hysteresis effects^{71,72}. Even though they usually concern long DNA chains, they may be due to local effects like slow ion diffusion especially under low hydration.

Our results feature the complexity of the poly(dA).poly(dT) DNA as regards the B/A polymorphism, but they leave unanswered the question concerning the main physical origin of such extraordinary behavior. A number of factors can contribute to the poly(dA).poly(dT) persistence with respect to the B→A transition. The sequence dependent propensities towards A and B-forms should certainly originate from the specific base stacking^{9,10,11}. However, the variety and the character of the observed environmental effects suggest that subtle structural deviations prompted by specific base-base contacts are amplified by strong interactions with water and counterions. For instance, the narrow minor groove profile in the B-form of poly(dA).poly(dT) may be sealed by the hydration spine structure⁷³. The same feature should produce a twofold effect upon the counterion distribution around DNA^{24,47}. The free positive ions should tend to accumulate in front of the narrow minor groove, and, simultaneously, their concentration in the major groove is reduced. Both these features should stabilize the B-form. Earlier experimental and computational observations also suggest that a special role should be played by thymine methyl groups. They hinder a negative slide movement involved in the B→A transition¹¹ and form a continuous non-polar cluster in the major groove of B-DNA that should provide additional hydrophobic stabilization³¹. The same feature effectively reduces the accessible volume of the major groove and can prevent accumulation of free

solvent cations²⁰.

Many years ago, the contrasting propensities of poly(dA).poly(dT) and poly(dG).poly(dC) DNA to adopt A- and B-forms presented the first experimental demonstration of sequence dependent properties of the double helical DNA structure⁷⁴. Since then the repertory of reported sequence effects has many times increased, and yet the exact physical origin of this particular difference remains controversial. It is shown here that A↔B transitions observed in water drop simulations exhibit clear trends qualitatively similar to the long known experimental observations. These results corroborate the putative general role of the intra-duplex electrostatic condensation mechanism for A↔B transitions in DNA *in vitro* and suggest that future studies in the same direction can give more definite answers to the issues discussed here.

Methods

A series of MD simulations was carried out for double helical dodecamer fragments poly(dA).poly(dT) and poly(dG).poly(dC) referred to as A12 and G12, respectively, as well as a few derivatives of these sequences. Water drops of 300, 400, 500, 600, 700, 800, 1000, and 2000 molecules were used, which gives approximate hydration numbers (water/nucleotide) 13, 17, 21, 25, 29, 33, 42, and 83, respectively. Additional simulations with a hydration number around 171 were carried out by using periodical boundary conditions. Below for brevity the simulation conditions outlined above are referred to as HN13, HN17, and so fourth. All calculations were continued long enough to obtain convergent average parameters of the final states. In this way a quasi-static pattern of B↔A transitions can be reproduced resembling *in vitro* titration experiments

The simulation protocols were similar to the earlier water drop simulations^{20,22}. We use the internal coordinate molecular dynamics (ICMD) method^{75,76} adapted for DNA^{77,78} with the time step of 0.01 ps. In this approach, the DNA molecule has all bond length and almost all bond angles fixed at their standard values. The only variable bond angles are those centered at the sugar C1',...,C4', and O4' atoms, which assures the flexibility of the furanose rings. In contrast, bases, thymine methyls, and phosphate groups move as articulated rigid bodies, with only rotations around single bonds allowed. The highest frequencies in thus obtained models are additionally balanced by increasing rotational inertia of the lightest rigid bodies as described earlier^{77,79}. The possible physical effects of the above modifications have been discussed elsewhere^{76,80}. The electrostatic interactions are treated with the recent version of the SPME method⁸¹ specifically adapted for infinite vacuum boundary conditions²². The common values of Ewald parameters were used, that is 9 Å truncation for the real space sum and $\beta \approx 0.35$. Reference simulations with periodical

boundaries were carried out as described before²², with the standard SPME method in NVT ensemble conditions with a rectangular unit cell of $45 \times 45 \times 65$ Å under normal water density.

The initial states were prepared as follows. The canonical A and B-DNA⁸² were used as standard initial conformations. The DNA molecule was first immersed in a large rectangular TIP3P⁸³ water box of and next external solvent molecules were removed by using a spherical distance cut-off from DNA atoms. The cut-off radius was adjusted to obtain the desired number of water molecules remaining. The drop was neutralized by randomly placing Na^+ ions at water positions selected so that their distances from DNA were 5 Å or larger. The initial counterion distribution was pre-equilibrated by running 1 ns dynamics in water drops of 500 molecules for A-DNA and 800 molecules for B-DNA, with DNA atoms weakly restrained to their initial positions. The final drop size was adjusted by adding or removing water from the surface.

The described procedure was intended to assure the start of dynamics from closely similar states regardless of the drop size.

Every system was energy minimized first with the solute held rigid and then with all degrees of freedom. Dynamics were initiated with the Maxwell distribution of generalized momenta at low temperature. The system was next slowly heated to 250 K and equilibrated during several picoseconds. Production trajectories were computed with the temperature bound to 293 K by the Berendsen algorithm⁸⁴ with a relaxation time of 10 ps. For better comparison with earlier simulations of $A \leftrightarrow B$ transitions, the original Cornell et al. force field⁶⁶ was used. Duration of production runs varied from 2 to 25 ns depending upon the observed character of dynamics. The conformations were saved with a 2.5 ps interval. The results were analyzed with in-house routines and the Curves program⁵⁵.

-
- ¹ Saenger, W. (1984). *Principles of Nucleic Acid Structure*, Springer-Verlag, New York.
 - ² Ivanov, V. I. & Minchenkova, L. E. (1995). The A-form of DNA: in search of biological role (a review). *Mol. Biol.* **28**, 780–788.
 - ³ Lu, X. J., Shakked, Z., & Olson, W. K. (2000). A-form conformational motifs in ligand-bound DNA structures. *J. Mol. Biol.* **300**, 819–840.
 - ⁴ Franklin, R. E. & Gosling, R. G. (1953). Molecular configuration in sodium thymonucleate. *Nature* **171**, 740–741.
 - ⁵ Leslie, A. G. W., Arnott, S., Chandrasekaran, R., & Ratliff, R. L. (1980). Polymorphism of DNA double helices. *J. Mol. Biol.* **143**, 49–72.
 - ⁶ Piškur, J. & Rupprecht, A. (1995). Aggregated DNA in ethanol solution. *FEBS Lett.* **375**, 174–178.
 - ⁷ Tunis-Schneider, M. J. & Maestre, M. F. (1970). Circular dichroism spectra of oriented and unoriented deoxyribonucleic acid films: A preliminary study. *J. Mol. Biol.* **52**, 521–541.
 - ⁸ Ivanov, V. I., Minchenkova, L. E., Minyat, E. E., Frank-Kametetskii, M. D., & Schyolkina, A. K. (1974). The B to A transition of DNA in solution. *J. Mol. Biol.* **87**, 817–833.
 - ⁹ Calladine, C. R. & Drew, H. R. (1984). A base-centered explanation of the B-to-A transition in DNA. *J. Mol. Biol.* **178**, 773–782.
 - ¹⁰ Mazur, J., Sarai, A., & Jernigan, R. L. (1989). Sequence dependence of the B-A conformational transition of DNA. *Biopolymers* **28**, 1223–1233.
 - ¹¹ Hunter, C. A. (1993). Sequence-dependent DNA structure. The role of base stacking interactions. *J. Mol. Biol.* **230**, 1025–1054.
 - ¹² Ivanov, V. I., Zhurkin, V. B., Zavriev, S. K., Lysov, Y. P., Minchenkova, L. E., Minyat, E. E., Frank-Kamenetskii, M. D., & Schyolkina, A. K. (1979). Conformational possibilities of double-helical nucleic acids: Theory and experiment. *Int. J. Quantum Chem.* **16**, 189–201.
 - ¹³ Cheatham, III, T. E. & Kollman, P. A. (1996). Observation of the A-DNA to B-DNA transition during unrestrained molecular dynamics in aqueous solution. *J. Mol. Biol.* **259**, 434–444.
 - ¹⁴ Yang, L. & Pettitt, B. M. (1996). B to A transition of DNA on the nanosecond time scale. *J. Phys. Chem. B* **100**, 2564–2566.
 - ¹⁵ Cheatham, III, T. E., Crowley, M. F., Fox, T., & Kollman, P. A. (1997). A molecular level picture of the stabilization of A-DNA in mixed ethanol-water solutions. *Proc. Natl. Acad. Sci. U.S.A.* **94**, 9626–9630.
 - ¹⁶ Cheatham, III, T. E. & Kollman, P. A. (1997). Insight into the stabilization of A-DNA by specific ion association: Spontaneous B-DNA to A-DNA transitions observed in molecular dynamics simulations of d[ACCCGCGGGT]2 in the presence of hexaamminecobalt(III). *Structure* **5**, 1297–1311.
 - ¹⁷ Cieplak, P., Cheatham, III, T. E., & Kollman, P. A. (1997). Molecular dynamics simulations find that 3'-phosphoramidate modified DNA duplexes undergo B to A transition and normal DNA duplexes an A to B transition. *J. Am. Chem. Soc.* **119**(29), 6722–6730.
 - ¹⁸ Jayaram, B., Sprous, D., Young, M. A., & Beveridge, D. L. (1998). Free energy analysis of the conformational preferences of A and B forms of DNA in solution. *J. Am. Chem. Soc.* **120**, 10629–10633.
 - ¹⁹ Sprous, D., Young, M. A., & Beveridge, D. L. (1998). Molecular dynamics studies of the conformational preferences of a DNA double helix in water and an ethanol/water mixture: Theoretical considerations of the A-B transition. *J. Phys. Chem. B* **102**, 4658–4667.
 - ²⁰ Mazur, A. K. (2003). Titration *in silico* of reversible $B \leftrightarrow A$ transitions in DNA. *J. Am. Chem. Soc.* **125**(26), 7849–7859.
 - ²¹ Feig, M. & Pettitt, B. M. (1998). Structural equilibrium of DNA represented with different force fields. *Biophys. J.* **75**, 134–149.
 - ²² Mazur, A. K. (2002). DNA dynamics in a water drop without counterions. *J. Am. Chem. Soc.* **124**(49), 14707–14715.
 - ²³ Feuerstein, B. G., Pattabiraman, N., & Marton, L. J. (1986). Spermine-DNA interactions: a theoretical study.

- Proc. Natl. Acad. Sci. U. S. A.* **83**, 5948–52.
- 24 Rouzina, I. & Bloomfield, V. A. (1998). DNA bending by small, mobile multivalent cations. *Biophys. J.* **74**, 3152–3164.
 - 25 Xu, Q., Shoemaker, R. K., & Braunlin, W. H. (1993). Induction of B-A transitions of deoxyoligonucleotides by multivalent cations in dilute aqueous solution. *Biophys. J.* **65**, 1039–1049.
 - 26 Saenger, W., Hunter, W. N., & Kennard, O. (1986). DNA conformation is determined by economics in the hydration of phosphate groups. *Nature* **324**, 385–388.
 - 27 Ivanov, V. I., Minchenkova, L. E., Schyolkina, A. K., & Poletaev, A. I. (1973). Different conformations of double-stranded nucleic acids in solution as revealed by circular dichroism. *Biopolymers* **12**, 89–110.
 - 28 Zimmerman, S. B. (1983). The three-dimensional structure of DNA. *Ann. Rev. Biochem.* **51**, 395–427.
 - 29 Becker, M. M. & Wang, Z. (1989). B->A transitions within a 5 S ribosomal RNA gene are highly sequence-specific. *J. Biol. Chem.* **265**, 4163–4167.
 - 30 Basham, B., Schroth, G. P., & Ho, P. S. (1995). An A-DNA triplet code: Thermodynamic rules for predicting A- and B-DNA. *Proc. Natl. Acad. Sci. U.S.A.* **92**, 6464–6468.
 - 31 Tolstorukov, M. Y., Ivanov, V. I., Malenkov, G. G., Jernigan, R. L., & Zhurkin, V. B. (2001). Sequence-dependent B-A transition in DNA evaluated with dimeric and trimeric scales. *Biophys. J.* **81**, 3409–3421.
 - 32 Peck, L. J. & Wang, J. C. (1981). Sequence dependence of the helical repeat of DNA in solution. *Nature* **292**, 375–378.
 - 33 Rhodes, D. & Klug, A. (1981). Sequence-dependent helical periodicity of DNA. *Nature* **292**, 378–380.
 - 34 Strauss, F., Gaillard, C., & Prunell, A. (1981). Helical periodicity of DNA, poly(dA).poly(dT) and poly(dA-dT).poly(dA-dT) in solution. *Eur. J. Biochem* **118**, 215–222.
 - 35 Hogan, M., LeGrange, J., & Austin, B. (1983). Dependence of DNA helix flexibility on base composition. *Nature* **304**, 752–754.
 - 36 Nishimura, Y., Torigoe, C., & Tsuboi, M. (1986). Salt induced B to A transition of poly(dG)-poly(dC) and the stabilization of A form by its methylation. *Nucleic Acids Res.* **14**, 2737–2749.
 - 37 Behling, R. W. & Kearns, D. R. (1986). ¹H two-dimensional nuclear Overhauser effect and relaxation studies of poly(dA).poly(dT). *Biochemistry* **25**, 3335–3346.
 - 38 Benevides, J. M., Wang, A. H., Rich, A., Kyogoku, Y., van der Marel, G. A., van Boom, J. H., & Thomas, Jr., G. J. (1986). Raman spectra of single crystals of r(GCG)d(CGC) and d(CCCGGG) as models for A DNA, their structure transitions in aqueous solution, and comparison with double-helical poly(dG).poly(dC). *Biochemistry* **25**, 41–50.
 - 39 Sarma, M. H., Gupta, G., & Sarma, R. H. (1986). 500-MHz ¹H NMR study of poly(dG).poly(dC) in solution using one-dimensional nuclear Overhauser effect. *Biochemistry* **25**, 3659–3665.
 - 40 Peticolas, W. L., Wang, Y., & Thomas, G. A. (1988). Some rules for predicting the base-sequence dependence of DNA conformation. *Proc. Natl. Acad. Sci. U.S.A.* **85**, 2579–2583.
 - 41 Buckin, V. A., Kankiya, B. I., Bulichov, N. V., Lebedev, A. V., Gukovsky, I. Y., Chuprina, V. P., Sarvazyan, A. P., & Williams, A. R. (1989). Measurement of anomalously high hydration of (dA)_n.(dT)_n double helices in dilute solution. *Nature* **340**, 321–322.
 - 42 Buckin, V. A., Kankiya, B. I., Sarvazyan, A. P., & Uedaira, H. (1989). Acoustical investigation of poly(dA).poly(dT), [poly[d(A-T)]], poly(A).poly(U) and DNA hydration in dilute aqueous solutions. *Nucleic Acids Res.* **17**, 4189–4203.
 - 43 Brahms, S., Fritsch, V., Brahms, J. G., & Westhof, E. (1992). Investigations on the dynamics structures of adenine- and thymine-containing DNA. *J. Mol. Biol.* **223**, 455–476.
 - 44 Chalikian, T. V., Plum, G. E., Sarvazyan, A. P., & Breslauer, K. J. (1994). Influence of drug binding on DNA hydration: acoustic and densimetric characterizations of netropsin binding to the poly(dAdT).poly(dAdT) and poly(dA).poly(dT) duplexes and poly(dT).poly(dA).poly(dT) triplex at 25 degrees C. *Biochemistry* **26**, 8629–8640.
 - 45 Vorlickova, M., Subriana, J. A., Chladkova, J., Tejralova, I., Huynh-Dinh, T., Arnold, L., & Kypr, J. (1986). Comparison of the solution and crystal conformations of (G+C)-rich fragments of DNA. *Biophys. J.* **71**, 1530–1538.
 - 46 Ivanov, V. I., Minchenkova, L. E., Burckhardt, G., Birch-Hirschfeld, E., Fritzsche, H., & Zimmer, C. (1996). The detection of B-form/A-form junction in a deoxyribonucleotide duplex. *Biophys. J.* **71**, 3344–3349.
 - 47 Hud, N. V. & Plavec, J. (2003). A unified model for the origin of DNA sequence-directed curvature. *Biopolymers* **69**, 144–159.
 - 48 Hud, N. V. & Polak, M. (2001). DNA-cation interactions: The major and minor grooves are flexible ionophores. *Curr. Opin. Struct. Biol.* **11**, 293–301.
 - 49 Dechering, K. J., Cuelenaere, K., Konings, R. N., & Leunissen, J. A. (1998). Distinct frequency-distributions of homopolymeric DNA tracts in different genomes. *Nucleic Acids Res.* **26**, 4056–4062.
 - 50 Trifonov, E. N. & Sussman, J. L. (1980). The pitch of chromatin DNA is reflected in its nucleotide sequence. *Proc. Natl. Acad. Sci. U.S.A.* **77**(7), 3816–3820.
 - 51 Widlund, H. R., Cao, H., Simonsson, S., Magnusson, E., Simonsson, T., Nielsen, P. E., Kahn, J. D., Crothers, D. D., & Kubista, M. (1997). Identification and characterization of genomic nucleosome-positioning sequences. *J. Mol. Biol.* **267**, 807–817.
 - 52 Vashakidze, R. P. & Prangishvili, D. A. (1987). Simple repetitive sequences in the genomes of archaebacteria. *FEBS Lett.* **216**, 217–220.
 - 53 Altona, C. & Sundaralingam, M. (1972). Conformational analysis of the sugar ring in nucleosides and nucleotides. A new description using the concept of pseudorotation. *J. Am. Chem. Soc.* **94**(23), 8205–8212.
 - 54 Mazur, A. K. (1999). Internal correlations in minor groove profiles of experimental and computed B-DNA conformations. *J. Mol. Biol.* **290**, 373–377.
 - 55 Lavery, R. & Sklenar, H. (1988). The definition of generalized helicoidal parameters and of axis curvature for irregular nucleic acids. *J. Biomol. Struct. Dyn.* **6**(1), 63–91.
 - 56 Minchenkova, L. E., Schyolkina, A. K., Chernov, B. K., & Ivanov, V. I. (1986). CC/GG contacts facilitate the B to A transition of DNA in solution. *J. Biomol. Struct. Dyn.* **4**, 463–476.
 - 57 The current AMBER parameters reportedly overestimate the stability of cytosine C2'-endo sugar pucker with respect to the C3'-endo⁶². This forcefield defect is perhaps responsible for a delayed transition of cytosine sugars to

- C3'-endo and it may somewhat reduce the A-philicity of poly(dG).poly(dC) DNA.
- ⁵⁸ The quasi-static profiles in our calculations should be distinguished from familiar S-shaped experimental plots of cooperative A \leftrightarrow B transitions⁸. In the latter case they result from two different contributions: (i) the shift in relative populations of A- and B-forms in the ensemble of DNA conformations, and (ii) small deformations of the A and B-conformations under varied hydration. Our simulations probe only the second contribution. Its relative weight in experiments is not known well. The Ising model of cooperative A \leftrightarrow B transitions considers only the first contribution⁸. The second one is effectively neglected by assuming that in small DNA fragments the transition is described by a step function. It is known, however, that, beyond the transition zone of hydration numbers, conformations of both B- and A-DNA change in a smooth and non-cooperative manner and that these changes are rather significant^{85,86}. Evaluation of equilibrium populations of A and B-forms from this types of simulations rests beyond the current possibilities, nevertheless, reversion of A \leftrightarrow B transitions in a single MD trajectory can be observed in very long simulations under intermediate hydration (unpublished results).
- ⁵⁹ Trantirek, L., Steff, R., Vorlickova, M., Koca, J., Sklenar, V., & Kypr, J. (2000). An A-type double helix of DNA having B-type puckering of the deoxyribose rings. *J. Mol. Biol.* **297**, 907–22.
- ⁶⁰ Steff, R., Trantirek, L., Vorlickova, M., Koca, J., Sklenar, V., & Kypr, J. (2001). A-like guanine-guanine stacking in the aqueous DNA duplex of d(GGGGCCCC). *J. Mol. Biol.* **307**, 513–24.
- ⁶¹ Lankas, F., Cheatham, III, T. E., Spaskova, N., Hobza, P., Langowskii, J., & Sponer, J. (2002). Critical effect of the N2 amino group on structure, dynamics, and elasticity of DNA polypurine tracts. *Biophys. J.* **82**, 2592–2609.
- ⁶² Cheatham, III, T. E., Cieplak, P., & Kollman, P. A. (1999). A modified version of the Cornell et al. force field with improved sugar pucker phases and helical repeat. *J. Biomol. Struct. Dyn.* **16**, 845–862.
- ⁶³ Ivanov, V. I., Krylov, D. Y., & Minyat, E. E. (1985). Three state diagram for DNA. *J. Biomol. Struct. Dyn.* **3**, 43–55.
- ⁶⁴ Vorlickova, M., Sagi, J., Hejtmankova, I., & Kypr, J. (1991). Alkyl substituent in place of the thymine methyl group controls the A-X conformational bimorphism in poly(dA-dT). *J. Biomol. Struct. Dyn.* **9**, 571–8.
- ⁶⁵ Suzuki, M., Amano, N., Kakinuma, J., & Tateno, M. (1997). Use of a 3D structure data base for understanding sequence-dependent conformational aspects of DNA. *J. Mol. Biol.* **274**, 421–35.
- ⁶⁶ Cornell, W. D., Cieplak, P., Bayly, C. I., Gould, I. R., Merz, K. M., Ferguson, D. M., Spellmeyer, D. C., Fox, T., Caldwell, J. W., & Kollman, P. A. (1995). A second generation force field for the simulation of proteins, nucleic acids and organic molecules. *J. Am. Chem. Soc.* **117**(19), 5179–5197.
- ⁶⁷ Wahl, M. C. & Sundaralingam, M. (1999). A-DNA duplexes in the crystal. In Stephen Neidle, (ed.), *Oxford Handbook of Nucleic Acid Structure*, pp. 117–144 Oxford University Press New York.
- ⁶⁸ Ling, H., Boudsocq, F., Woodgate, R., & Yang, W. (2001). Crystal structure of a Y-family DNA polymerase in action: a mechanism for error-prone and lesion-bypass replication. *Cell*. **107**, 91–102.
- ⁶⁹ Arnott, S. & Selsing, E. (1974). Letter: The structure of polydeoxyguanylic acid with polydeoxycytidylic acid. *J. Mol. Biol.* **88**, 551–2.
- ⁷⁰ McConnell, K. J. & Beveridge, D. L. (2001). Molecular dynamics simulations of B'-DNA: Sequence effects on A-trait-induced bending and flexibility. *J. Mol. Biol.* **314**, 23–40.
- ⁷¹ Falk, M., Hartman, Jr., K. A., & Lord, R. C. (1962). Hydration of deoxyribonucleic acid. I. A gravimetric study. *J. Am. Chem. Soc.* **84**, 3843–3846.
- ⁷² Lindsay, S. M., Lee, S. A., Powell, J. W., Weidlich, T., Demarco, C., Lewen, G. D., Tao, N. J., & Rupprecht, A. (1988). The origin of the A to B transition in DNA fibers and films. *Biopolymers* **27**, 1015–1043.
- ⁷³ Dickerson, R. E., Drew, H. R., Conner, B. N., Wing, R. M., Fratini, A. V., & Kopka, M. L. (1982). The anatomy of A-, B-, and Z-DNA. *Science* **216**, 475–485.
- ⁷⁴ Pilet, J., Blicharski, J., & Brahms, J. (1975). Conformations and structural transitions in polydeoxynucleotides. *Biochemistry* **14**, 1869–76.
- ⁷⁵ Mazur, A. K. (1997). Quasi-Hamiltonian equations of motion for internal coordinate molecular dynamics of polymers. *J. Comput. Chem.* **18**(11), 1354–1364.
- ⁷⁶ Mazur, A. K. (2001). Internal coordinate simulation method. In Oren M. Becker, Alexander D. MacKerell, Jr., Benoit Roux, & Masakatsu Watanabe, (ed.), *Computational Biochemistry and Biophysics*, pp. 115–131 Marcel Dekker New York.
- ⁷⁷ Mazur, A. K. (1998). Accurate DNA dynamics without accurate long range electrostatics. *J. Am. Chem. Soc.* **120**(42), 10928–10937.
- ⁷⁸ Mazur, A. K. (1999). Symplectic integration of closed chain rigid body dynamics with internal coordinate equations of motion. *J. Chem. Phys.* **111**(4), 1407–1414.
- ⁷⁹ Mazur, A. K. (1998). Hierarchy of fast motions in protein dynamics. *J. Phys. Chem. B* **102**(2), 473–479.
- ⁸⁰ Mazur, A. K., Sumpter, B. G., & Noid, D. W. (2001). Internal coordinate phase space analysis of macromolecular systems. *Comput. Theor. Polym. Sci.* **11**(1), 35–47.
- ⁸¹ Essmann, U., Perera, L., Berkowitz, M. L., Darden, T., Lee, H., & Pedersen, L. G. (1995). A smooth particle mesh Ewald method. *J. Chem. Phys.* **103**, 8577–8593.
- ⁸² Arnott, S. & Hukins, D. W. L. (1972). Optimised parameters for A-DNA and B-DNA. *Biochem. Biophys. Res. Commun.* **47**, 1504–1509.
- ⁸³ Jorgensen, W. L., Chandreskhar, J., Madura, J. D., Impey, R. W., & Klein, M. L. (1983). Comparison of simple potential functions for simulating liquid water. *J. Chem. Phys.* **79**, 926–935.
- ⁸⁴ Berendsen, H. J. C., Postma, J. P. M., van Gunsteren, W. F., DiNola, A., & Haak, J. R. (1984). Molecular dynamics with coupling to an external bath. *J. Chem. Phys.* **81**, 3684–3690.
- ⁸⁵ Lee, C.-H., Mizusawa, H., & Kakefuda, T. (1981). Unwinding of double-stranded DNA helix by dehydration. *Proc. Natl. Acad. Sci. U.S.A.* **78**, 2838–2842.
- ⁸⁶ Harmouchi, M., Albiser, G., & Premilat, S. (1990). Changes of hydration during conformational transitions of DNA. *Eur. Biophys. J.* **19**, 87–92.